GPCR SIGNALING

Purinergic $P2Y_6$ receptors heterodimerize with angiotensin AT1 receptors to promote angiotensin II–induced hypertension

Akiyuki Nishimura,[1,2]* Caroline Sunggip,[1,3,4]* Hidetoshi Tozaki-Saitoh,[5,6] Tsukasa Shimauchi,[1,4] Takuro Numaga-Tomita,[1,2] Katsuya Hirano,[7] Tomomi Ide,[8] Jean-Marie Boeynaems,[9] Hitoshi Kurose,[10] Makoto Tsuda,[6] Bernard Robaye,[9] Kazuhide Inoue,[5] Motohiro Nishida[1,2,4,11]†

The angiotensin (Ang) type 1 receptor (AT1R) promotes functional and structural integrity of the arterial wall to contribute to vascular homeostasis, but this receptor also promotes hypertension. In our investigation of how Ang II signals are converted by the AT1R from physiological to pathological outputs, we found that the purinergic $P2Y_6$ receptor ($P2Y_6R$), an inflammation-inducible G protein (heterotrimeric guanine nucleotide–binding protein)–coupled receptor (GPCR), promoted Ang II–induced hypertension in mice. In mice, deletion of $P2Y_6R$ attenuated Ang II–induced increase in blood pressure, vascular remodeling, oxidative stress, and endothelial dysfunction. AT1R and $P2Y_6R$ formed stable heterodimers, which enhanced G protein–dependent vascular hypertrophy but reduced β-arrestin–dependent AT1R internalization. Pharmacological disruption of AT1R-$P2Y_6R$ heterodimers by the $P2Y_6R$ antagonist MRS2578 suppressed Ang II–induced hypertension in mice. Furthermore, $P2Y_6R$ abundance increased with age in vascular smooth muscle cells. The increased abundance of $P2Y_6R$ converted AT1R-stimulated signaling in vascular smooth muscle cells from β-arrestin–dependent proliferation to G protein–dependent hypertrophy. These results suggest that increased formation of AT1R-$P2Y_6R$ heterodimers with age may increase the likelihood of hypertension induced by Ang II.

INTRODUCTION

Hypertension is a major risk factor of various diseases including stroke, heart failure, vascular disease, and kidney disease. Angiotensin II (Ang II), which is produced by the renin-angiotensin system, primarily functions as a physiological regulator of blood pressure and cardiovascular homeostasis, but it also plays a major role in the pathogenesis of hypertension (*1*). In the aorta, Ang II promotes hypertrophy of vascular smooth muscle cells, resulting in hypertension by increasing arterial wall thickness and vascular resistance, a process called vascular remodeling (*2*). Additionally, Ang II induces physiological proliferation (a process called hyperplasia) of vascular smooth muscle cells. Pharmacological studies suggest that Ang II is involved in neointimal hyperplasia after vessel injury (*2*, *3*). Ang II has hyperplastic effects in the newborn and in the neointima, but not in adult vascular smooth muscle cells (*4*). The responsiveness of the artery to Ang II depends on age in rats (*5*, *6*). However, how vascular smooth muscle cells determine the responsiveness to Ang II under different developmental and region-specific conditions is mostly unclear.

Ang II binds to two types of G protein (heterotrimeric guanine nucleotide–binding protein)–coupled receptors (GPCRs) called angiotensin II type 1 receptor (AT1R) and AT2R (*7*). Although both receptors are found in vascular smooth muscle cells, AT1R accounts for most cardiovascular effects of Ang II (*8*, *9*). AT1R is primarily coupled with heterotrimeric $G_{q/11}$ protein to induce intracellular Ca^{2+} mobilization through phospholipase C activation, and with $G_{12/13}$ protein to activate Rho-dependent signaling. After GPCR stimulation, β-arrestin (βArr) is recruited to the cell membrane and triggers GPCR internalization to attenuate G protein–dependent signaling. In addition to receptor desensitization, βArr itself can mediate G protein–independent signaling (*10*, *11*). Ang II activates various signaling molecules, including mitogen-activated protein kinases and Akt, through G protein– and βArr-dependent pathways (*12*, *13*). Although biochemical studies demonstrate that GPCRs transmit signals as monomeric entries (*14*, *15*), many GPCRs probably exist as homo- and heterodimers in living cells (*15*). Receptor dimerization modulates receptor properties, including maturation and plasma membrane trafficking of nascent receptors, ligand binding, G protein selectivity, downstream signaling, and internalization (*16*). Heterodimerization between different GPCRs increases the diversity of signaling pathways activated by GPCRs and their regulation. AT1R heterodimerizes with various other GPCRs (*17*–*23*), suggesting cross-regulation between angiotensin II and other signaling pathways. The fourth to sixth transmembrane domain is expected to participate in heterodimerization (*24*), and the DRY ligand-binding motif of AT1R appears to be critical for functional activation of oligomerized AT1R signaling (*25*).

[1]Division of Cardiocirculatory Signaling, Okazaki Institute for Integrative Bioscience (National Institute for Physiological Sciences), National Institutes of Natural Sciences, Okazaki, Aichi 444-8787, Japan. [2]SOKENDAI (School of Life Science, The Graduate University for Advanced Studies), Hayama, Kanagawa 240-0193, Japan. [3]Department of Biomedical Science and Therapeutic, Faculty of Medicine and Health Sciences, Universiti Malaysia Sabah, Kota Kinabalu, Sabah 88400 Malaysia. [4]Department of Translational Pharmaceutical Sciences, Graduate School of Pharmaceutical Sciences, Kyushu University, Fukuoka 812-8582, Japan. [5]Department of Molecular and System Pharmacology, Graduate School of Pharmaceutical Sciences, Kyushu University, Fukuoka 812-8582, Japan. [6]Department of Life Innovation, Graduate School of Pharmaceutical Sciences, Kyushu University, Fukuoka 812-8582, Japan. [7]Department of Cardiovascular Physiology, Faculty of Medicine, Kagawa University, Kagawa 761-0793, Japan. [8]Department of Cardiovascular Medicine, Graduate School of Medical Sciences, Kyushu University, Fukuoka 812-8582, Japan. [9]Institute of Interdisciplinary Research, School of Medicine, Université Libre de Bruxelles, Gosselies 6041, Belgium. [10]Department of Pharmacology and Toxicology, Graduate School of Pharmaceutical Sciences, Kyushu University, Fukuoka 812-8582, Japan. [11]Precursory Research for Embryonic Science and Technology, Japan Science and Technology Agency, Kawaguchi, Saitama 332-0012, Japan.
*These authors contributed equally to this work.
†Corresponding author. E-mail: nishida@nips.ac.jp

Purinergic P2Y receptors are a family of GPCRs that respond to extracellular mononucleotides (*26*). Eight different subtypes of P2Y receptors ($P2Y_1R$, $P2Y_2R$, $P2Y_4R$, $P2Y_6R$, $P2Y_{11}R$, $P2Y_{12}R$, $P2Y_{13}R$, and $P2Y_{14}R$) have been identified in mammals and show marked differences in ligand selectivity and specificity of G protein coupling (*27*). After mechanical stress (*28*) or cellular injury (*29*), mononucleotides released from nonsecretory tissues may signal in an autocrine or paracrine manner to regulate biological functions. Additionally, dinucleotide phosphates, such as Up_4A and Ap_nA, are ligands that activate vasoregulatory processes (*30*, *31*) and may activate purinergic receptors (*32*). Multiple P2Y receptor subtypes, including $P2Y_6R$ (*33*, *34*), are present in blood vessels. G_q-coupled $P2Y_6R$ has strong ligand selectivity for UDP (uridine 5′-diphosphate) and shows a ubiquitous distribution in mammalian tissues. $P2Y_6R$ activation induces a Ca^{2+} response in vascular smooth muscle cells that results in contraction of isolated blood vessels (*26*). These pharmacological studies suggest that $P2Y_6R$ plays an important role in cardiovascular function. Although $P2Y_6R$ knockout mice do not show abnormalities of the cardiovascular system under normal conditions (*35*), $P2Y_6R$ ablation attenuates vascular inflammation in vivo under pathological conditions (*36*, *37*). These results suggest that $P2Y_6R$ participates in the development of pathological vascular remodeling.

We have previously shown that $P2Y_6R$ mediates pressure overload–induced cardiac fibrosis in mice (*38*). Mechanical stretch–induced nucleotides release initiates Rho-dependent fibrotic gene expressions in cardiomyocytes. Therefore, $P2Y_6R$-$G_{12/13}$ signaling is speculated to act as an upstream mediator of Ang II–AT1R signaling to induce fibrosis. Here, we investigated whether $P2Y_6R$ contributes to Ang II–induced pathophysiological functions through functional coupling with AT1R.

RESULTS

$P2Y_6R$ deletion attenuates Ang II–induced vascular remodeling in mice

To investigate the contribution of $P2Y_6R$ in Ang II–induced chronic hypertension, we measured blood pressures of $P2Y_6R$ knockout [$P2Y_6R^{(-/-)}$] and littermate control [$P2Y_6R^{(+/+)}$] mice infused with Ang II for 4 weeks. Mice of either genotype developed robust hypertension with Ang II treatment, but mean blood pressure of $P2Y_6R^{(-/-)}$ mice was significantly lower than that of $P2Y_6R^{(+/+)}$ mice (Fig. 1A). Heart rate was similar in $P2Y_6R^{(+/+)}$ and $P2Y_6R^{(-/-)}$ mice (Fig. 1B). Ang II treatment increased the medial cross-sectional area and wall-to-lumen ratio in both genotypes, but to a significantly lesser extent in $P2Y_6R^{(-/-)}$ mice (Fig. 1, C to E). Additionally, Ang II infusion significantly increased vascular fibrosis of $P2Y_6R^{(+/+)}$ mice, which was markedly suppressed in $P2Y_6R^{(-/-)}$ mice (Fig. 1F). Generation of reactive oxygen species (ROS) is required for Ang II–induced vascular hypertrophy (*13*), and 4-hydroxyl-2-nonenal (4-HNE) is a major membrane lipid peroxidation product and marker of oxidative stress (*39*). We found that Ang II–induced accumulation of 4-HNE adducts in aortae was greatly suppressed in $P2Y_6R^{(-/-)}$ mice compared with $P2Y_6R^{(+/+)}$ mice (Fig. 1G). These results suggest that deletion of $P2Y_6R$ in mice substantially protects tissues against the pathological effect of Ang II.

Ang II–induced vascular contraction is reduced in $P2Y_6R^{(-/-)}$ mice

We next examined whether $P2Y_6R$ contributes to Ang II–induced vascular dysfunction using isolated abdominal aortic rings. We first confirmed the effect of long-term Ang II treatment on endothelium-dependent relaxation evoked by UDP, an endothelium-dependent relaxing factor (*40*). UDP treatment induced vascular relaxation in a concentration-dependent manner, and the aortae from Ang II–infused mice showed inhibited UDP-evoked relaxation (Fig. 1H). The aortae from $P2Y_6R^{(-/-)}$ and $P2Y_6R^{(+/+)}$ mice showed similar UDP-evoked relaxation, suggesting that UDP induced endothelial-dependent relaxation through other P2Y receptors. Ang II pretreatment impaired UDP-induced relaxation to a lesser extent in $P2Y_6R^{(-/-)}$ aortae than in $P2Y_6R^{(+/+)}$ aortae (Fig. 1I). Moreover, Ang II– but not norepinephrine-induced contraction was significantly lower in aortae from $P2Y_6R^{(-/-)}$ mice compared with those from $P2Y_6R^{(+/+)}$ mice (Fig. 1, J and K), which suggested that AT1R-stimulated signaling was reduced in $P2Y_6R^{(-/-)}$ mice.

$P2Y_6R$ participates in the Ang II–induced Ca^{2+} response of vascular smooth muscle cells

Because Ang II–induced medial hypertrophy and contraction were impaired in blood vessels isolated from $P2Y_6R^{(-/-)}$ mice (Fig. 1, C and J), we next compared the AT1R response in isolated vascular smooth muscle cells. The intracellular Ca^{2+} response induced by $P2Y_6R$-specific agonist 3-phenacyl UDP (3-pUDP) was absent in vascular smooth muscle cells isolated from $P2Y_6R^{(-/-)}$ mice (Fig. 2A). *AT1R* mRNA expression was not significantly different between $P2Y_6R^{(+/+)}$ and $P2Y_6R^{(-/-)}$ vascular smooth muscle cells (Fig. 2B). However, the intracellular Ca^{2+} response induced by Ang II was reduced in $P2Y_6R^{(-/-)}$ cells (Fig. 2C). Furthermore, retroviral expression of mouse $P2Y_6R$–IRES (internal ribosomal entry site)–GFP (green fluorescent protein) into $P2Y_6R^{(-/-)}$ cells led to a higher Ca^{2+} response compared with GFP-expressing $P2Y_6R^{(-/-)}$ cells (Fig. 2D). These results suggested that $P2Y_6R$ promoted Ang II–induced G protein signaling in vascular smooth muscle cells.

$P2Y_6R$ heterodimerizes with AT1R

Heterodimerization modulates the function of several GPCRs (*16*). To determine whether $P2Y_6R$ heterodimerizes with AT1R, we used a bioluminescence resonance energy transfer (BRET) assay in cells expressing different ratios of AT1R-Rluc (donor) and $P2Y_6R$–YFP (yellow fluorescent protein) (acceptor) or YFP as a negative control. The BRET signal was saturated in cells expressing AT1R-Rluc and $P2Y_6R$-YFP, but not in the AT1R-Rluc and YFP (Fig. 3A). Moreover, overexpression of FLAG-$P2Y_6R$ as a competitor inhibited BRET signaling between AT1R-Rluc and $P2Y_6R$-YFP in a concentration-dependent manner (Fig. 3B). This finding suggested a specific interaction between $P2Y_6R$ and AT1R. Myc-$P2Y_6R$ coimmunoprecipitated with FLAG-AT1R in human embryonic kidney (HEK) 293 cells (Fig. 3C). Moreover, endogenous $P2Y_6R$ coimmunoprecipitated with endogenous AT1R in rat aortae (Fig. 3D), which suggested that these proteins formed a stable heterodimer.

$P2Y_6R$ binding prevents Ang II–induced desensitization of AT1R

βArr-dependent internalization of ligand-activated GPCR is important for receptor desensitization and turning off classical GPCR signaling (*10*, *11*). AT1R-YFP was mainly localized at the plasma membrane under basal conditions. After Ang II treatment, AT1R-YFP was localized to endosomes, which suggested that ligand-trigged receptor internalization had occurred (Fig. 3E). Myc-$P2Y_6R$ was colocalized with AT1R-YFP at the plasma membrane under basal conditions. However, coexpression of $P2Y_6R$ partially inhibited internalization of AT1R in response to Ang II (Fig. 3, F and G). We used BRET to measure Ang II–triggered βArr recruitment to AT1R in HEK293 expressing AT1R-Rluc and βArr2-YFP. Ang II stimulation increased the BRET signal between AT1R-Rluc and βArr2-YFP. This response was reduced by overexpression of $P2Y_6R$, which suggested that $P2Y_6R$ prevented Ang II–triggered βArr2 recruitment (Fig. 3H). We then captured the transient interaction of βArr2 with AT1R by cross-linking immunoprecipitation. Ang II–induced coimmunoprecipitation of βArr2-YFP with FLAG-AT1R was mostly inhibited by myc-$P2Y_6R$ expression, suggesting

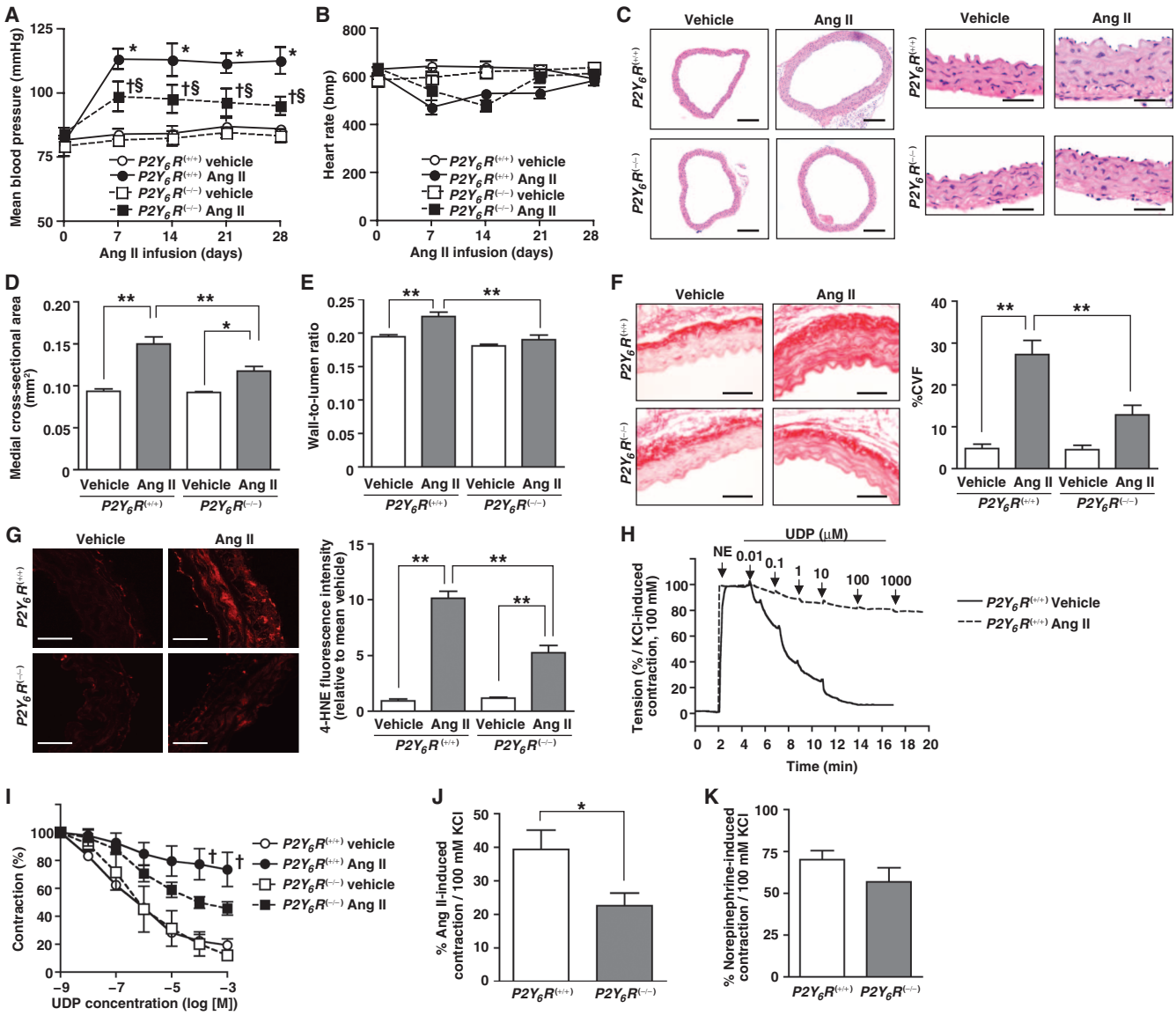

Fig. 1. P2Y$_6$R deletion attenuates Ang II–induced vascular remodeling in mice. (**A** and **B**) Mean blood pressure (MBP) (A) and heart rate (B) of *P2Y$_6$R$^{(+/+)}$* and *P2Y$_6$R$^{(−/−)}$* mice treated with Ang II or vehicle (n = 8 mice per genotype and treatment; $^*P < 0.05$ compared with *P2Y$_6$R$^{(+/+)}$* mice with vehicle, $^{\S}P < 0.05$ compared with *P2Y$_6$R$^{(−/−)}$* mice with vehicle, $^{\dagger}P < 0.05$ compared with *P2Y$_6$R$^{(+/+)}$* mice with Ang II). bpm, beats per minute. (**C** to **E**) Hematoxylin and eosin (H&E)–stained images of descending aortae. Right panels show magnified images (C). Scale bars, 200 μm (left) and 50 μm (right). Quantification of the medial cross-sectional area (D) and wall-to-lumen ratio (E) of descending aortae (n = 4 mice per genotype and treatment). $^{**}P < 0.01$, $^*P < 0.05$. (**F**) Picrosirius red–stained images of descending aortae. CVF, collagen volume fraction. Scale bars, 50 μm (n = 4 mice per genotype and treatment). $^{**}P < 0.01$. (**G**) Fluorescence images of 4-HNE adducts in abdominal aortae (n = 6 mice per genotype and treatment). Scale bars, 50 μm. $^{**}P < 0.01$. (**H**) Endothelium-dependent vasorelaxation induced by UDP. The abdominal aorta from *P2Y$_6$R$^{(+/+)}$* mice with Ang II or vehicle was precontracted by norepinephrine (NE) (n = 3 mice per genotype and treatment). (**I**) Concentration-dependent vasorelaxation induced by UDP in abdominal aortae from *P2Y$_6$R$^{(+/+)}$* and *P2Y$_6$R$^{(−/−)}$* mice with Ang II or vehicle (n = 3 mice per genotype and treatment). Kruskal-Wallis test followed by Dunn's post hoc test. $^{\dagger}P < 0.05$ compared with *P2Y$_6$R$^{(+/+)}$* mice with vehicle. (**J** and **K**) Peak constriction induced by Ang II (J) or NE (K) in abdominal aortae from mice [n = 6 (J) or n = 4 (K) mice per genotype]. $^*P < 0.05$, Mann-Whitney test.

that AT1R-P2Y$_6$R heterodimerization inhibited ligand-triggered recruitment of βArr2 (Fig. 3I). After βArr is recruited to activated GPCR, the GPCR-βArr complex is internalized. βArr2-YFP translocated from the cytosol to the intracellular puncta after Ang II treatment (Fig. 3J), a response that was inhibited by expression of P2Y$_6$R (Fig. 3K).

We next tested whether endogenous P2Y$_6$R participates in preventing desensitization of AT1R. Ang II–induced internalization of βArr2-YFP was greater in vascular smooth muscle cells from *P2Y$_6$R$^{(−/−)}$* mice than in those from *P2Y$_6$R$^{(+/+)}$* mice (Fig. 3, L and M). Ang II–induced AT1R internalization, as assessed by the BRET signals between AT1R-Rluc and Venus-PM

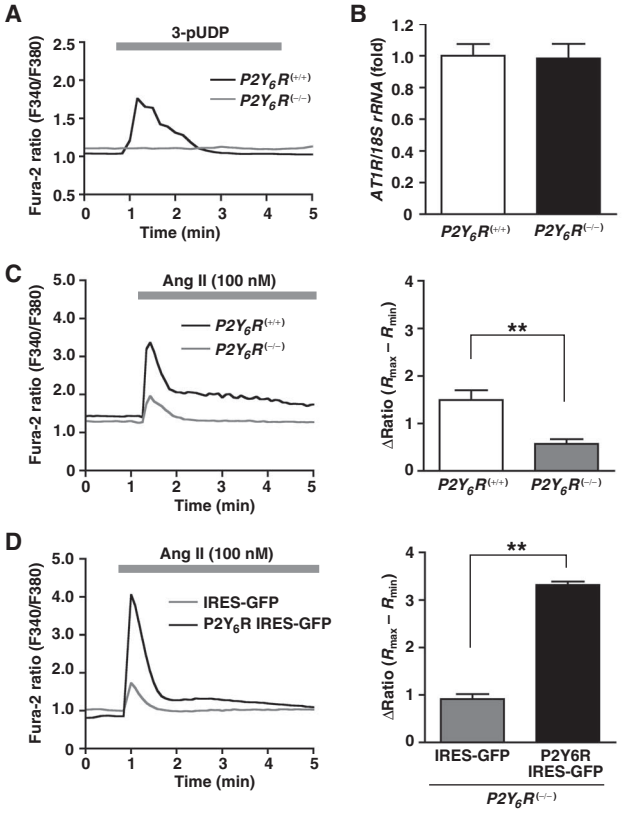

Fig. 2. $P2Y_6R$ participates in Ang II–induced Ca^{2+} response of mouse vascular smooth muscle cells (VSMCs). (**A**) Average traces of Ca^{2+} responses in VSMCs induced by 3-pUDP ($n = 3$ independent experiments; VSMCs were isolated from three mice per genotype). (**B**) *AT1R* mRNA expression in VSMCs isolated from $P2Y_6R^{(+/+)}$ and $P2Y_6R^{(-/-)}$ mice ($n = 3$ independent experiments; VSMCs were isolated from three mice per genotype). (**C**) Representative traces of Ca^{2+} responses in VSMCs induced by Ang II. Right panel: Peak $[Ca^{2+}]_i$ increases (ΔRatio) induced by Ang II ($n = 5$ independent experiments; VSMCs were isolated from three mice per genotype). $^{**}P < 0.01$. (**D**) Representative traces of Ang II–induced Ca^{2+} responses in $P2Y_6R^{(-/-)}$ VSMCs infected with retroviruses encoding *IRES-GFP* or *P2Y6R-IRES-GFP*. Right panel: ΔRatio ($n = 3$ independent experiments; VSMCs were isolated from three mice). $^{**}P < 0.01$.

(a plasma membrane–localized fluorophore), was not altered in $P2Y_6R^{(+/+)}$ vascular smooth muscle cells. In contrast, Ang II treatment significantly reduced the BRET signal in $P2Y_6R^{(-/-)}$ vascular smooth muscle cells (Fig. 3N), an effect that was significantly abolished by βArr2 knockdown (fig. S1). These results suggest that endogenous $P2Y_6R$ prevents βArr (mainly βArr2)–dependent desensitization of AT1R, resulting in enhanced G protein–dependent signaling.

Disruption of the AT1R-$P2Y_6R$ heterodimer by MRS2578 inhibits Ang II–induced hypertension

We use the noncompetitive $P2Y_6R$-selective antagonist MRS2578 to further test whether $P2Y_6R$ activity affected heterodimer formation (*41*). MRS2578 impaired coimmunoprecipitation of myc-$P2Y_6R$ with FLAG-AT1R in a concentration-dependent manner in vascular smooth muscle cells (Fig. 4A). The BRET signal between AT1R-Rluc and $P2Y_6R$-YFP was also reduced by MRS2578, which suggested that MRS2578 binding to $P2Y_6R$ inhibited heterodimer formation of AT1R-$P2Y_6R$ (Fig. 4B). Consistent with these results, MRS2578 promoted Ang II–induced internalization of AT1R in $P2Y_6R^{(+/+)}$ vascular smooth muscle cells (fig. S2A). In contrast, the AT1R antagonist losartan did not affect AT1R-$P2Y_6R$ heterodimer formation (fig. S2B). UDP concentrations in plasma were unchanged in Ang II–infused mice, and 3-pUDP binding had no effect on AT1R-$P2Y_6R$ heterodimer formation and AT1R internalization (fig. S2, C to E). Dinucleotide phosphates, such as Up_4A, are ligands of various P2Y receptors (*30*, *32*). We found that Up_4A activated $P2Y_6R$ in $P2Y_6R$-overexpressing HeLa cells (fig. S3A). However, Up_4A did not affect AT1R-$P2Y_6R$ heterodimer formation (fig. S2D) and Up_4A-induced Ca^{2+} responses were not different between $P2Y_6R^{(+/+)}$ and $P2Y_6R^{(-/-)}$ vascular smooth muscle cells (fig. S3B). These findings indicate that $P2Y_6R$ may not participate in Up_4A-induced responses in vascular smooth muscle cells.

The Ang II–induced intracellular Ca^{2+} increase and ROS generation were partially suppressed by pretreatment with MRS2578 in vascular smooth muscle cells (Fig. 4, C and D). MRS2578 did not affect basal blood pressure, but significantly inhibited the Ang II–induced sustained increase in blood pressure (Fig. 4E). Additionally, MRS2578 suppressed Ang II–induced vascular hypertrophy as demonstrated by an increase in the medial cross-sectional area of mouse thoracic aorta (Fig. 4F). These results suggested that heterodimer formation of AT1R and $P2Y_6R$ participated in Ang II–mediated vascular hypertrophy in vivo and that MRS2578 suppressed Ang II–induced hypertension by disrupting heterodimer formation.

A developmentally induced increase in $P2Y_6R$ abundance alters Ang II responses of vascular smooth muscle cells

Because Ang II triggers different cellular responses in neonatal and adult vascular smooth muscle cells (*4*), we investigated whether age-dependent changes in $P2Y_6R$ abundance determine the response of vascular smooth muscle cells to Ang II. *$P2Y_6R$* mRNA expression was higher in P30 vascular smooth muscle cells than in E17 or P1 vascular smooth muscle cells (Fig. 5A). Consistent with this finding, ERK (extracellular signal–regulated kinase) activation induced by the $P2Y_6R$-specific agonist 3-pUDP was greater in P30 vascular smooth muscle cells than in P1 vascular smooth muscle cells (Fig. 5B and fig. S4). In contrast, although Ang II–triggered Akt activation was enhanced in P30 vascular smooth muscle cells (Fig. 5C), Ang II–induced ERK activation was similar in vascular smooth muscle cells at different developmental stages (Fig. 5D). G_q inhibitory peptide blocked Ang II–induced Akt activation (fig. S5), consistent with the involvement of $G_q\alpha$-mediated Ca^{2+} mobilization in this process (*12*). This finding suggested that G_q-mediated signaling was potentiated in P30 vascular smooth muscle cells. Ang II–stimulated AT1R activates not only G protein–dependent but also βArr-dependent signaling pathways (*10*, *11*). [Sar(1), Ile(4), Ile(8)]Ang II (S II), a biased AT1R agonist that selectively activates βArr-dependent pathways, did not activate Akt or ERK in P30 vascular smooth muscle cells (Fig. 5, E and F). Knockdown of βArr1 and βArr2 had no effect on Ang II–induced Akt and ERK activation in P30 vascular smooth muscle cells (fig. S6A). However, S II induced activation of ERK, but not that of Akt, in E17 vascular smooth muscle cells (Fig. 5, E and F), and ERK activation was partially suppressed by βArr1/2 knockdown (fig. S6B). These results suggested that βArr partially mediated Ang II–induced ERK activation in E17 neonatal vascular smooth muscle cells but that Ang II–induced Akt and ERK activation was G protein–dependent in P30 adult vascular smooth muscle cells.

We next examined the biological importance of G protein– and βArr-dependent signals. Ang II treatment in P30, but not P1, vascular smooth muscle cells enhanced hypertrophic growth (Fig. 5G) as well as abundance of smooth muscle myosin heavy chain (SM-MHC), which encodes a marker of the mature contractile phenotype (fig. S7) (*42*). Activation of p70 ribosomal

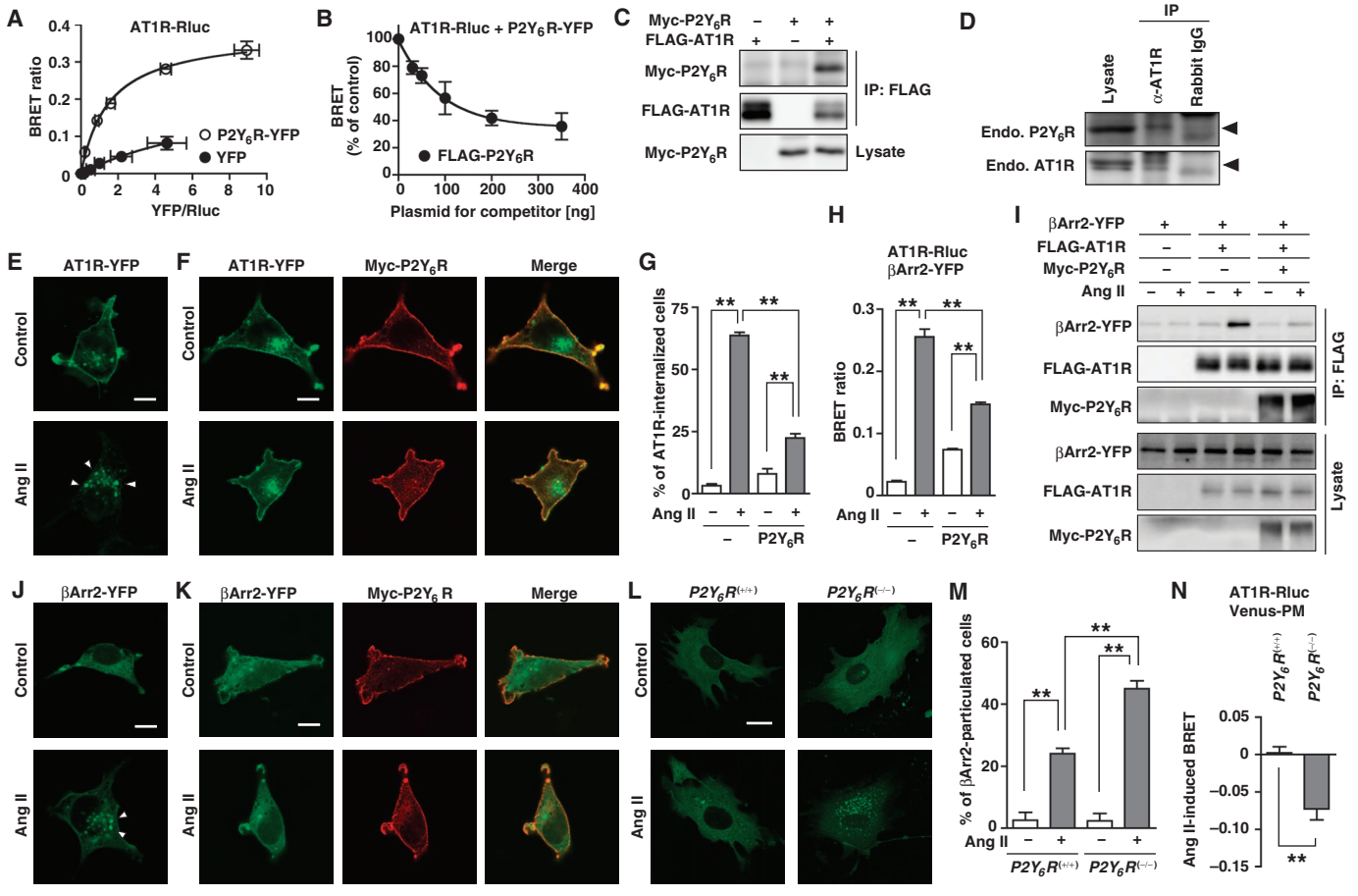

Fig. 3. The AT1R-P2Y$_6$R heterodimer prevents Ang II–induced AT1R internalization. (**A**) BRET saturation assay between AT1R-Rluc (donor) and P2Y$_6$R-YFP (acceptor) in HEK293 cells. YFP was used as a negative control (n = 3 independent experiments). (**B**) BRET competition assay between AT1R-Rluc and P2Y$_6$R-YFP with an increasing amount of FLAG-P2Y$_6$R (n = 3 independent experiments). (**C**) Interaction between FLAG-AT1R and myc-P2Y$_6$R in HEK293 cells (n = 3 independent experiments). IP, immunoprecipitation. (**D**) Interaction between endogenous AT1R and endogenous P2Y$_6$R in rat aortae (n = 3 independent experiments). (**E** to **G**) HEK293 cells expressing AT1R-YFP alone (E) or both AT1R-YFP and myc-P2Y$_6$R (F) with or without Ang II. Arrowheads show internalized AT1R-YFP. Scale bars, 10 μm. Quantification (G) of AT1R-internalized cells (n = 3 independent experiments). $^{**}P < 0.01$. (**H**) BRET ratio calculated from cells expressing AT1R-Rluc and βArr2-YFP with or without FLAG-P2Y$_6$R (n = 3 independent experiments). $^{**}P < 0.01$. (**I**) Interaction of βArr2-YFP with FLAG-AT1R with or without Ang II (n = 3 independent experiments). (**J** and **K**) HEK293 cells expressing AT1R-Rluc and βArr2-YFP without (J) or with FLAG-P2Y$_6$R (K). Arrowheads show internalized βArr2-YFP. Scale bars, 10 μm (n = 3 independent experiments). (**L** and **M**) Ang II–induced βArr2-YFP internalization in *P2Y$_6$R*$^{(+/+)}$ and *P2Y$_6$R*$^{(-/-)}$ VSMCs. Scale bars, 20 μm. Quantitative result (M) of βArr2-particulated cells (n = 3 independent experiments; VSMCs were isolated from three mice per genotype). $^{**}P < 0.01$. (**N**) Changes in the BRET ratio between AT1R-Rluc and Venus-PM in *P2Y$_6$R*$^{(+/+)}$ or *P2Y$_6$R*$^{(-/-)}$ VSMCs in the presence or absence of Ang II (n = 5 independent experiments; VSMCs were isolated from three mice per genotype). $^{**}P < 0.01$.

S6 kinase (p70S6K), a major regulator of vascular hypertrophy (*43*), was enhanced in P30 adult vascular smooth muscle cells (Fig. 5H). Ang II–induced increases in p70S6K activation and protein synthesis (as assessed by [^{3}H]leucine incorporation) were significantly suppressed by inhibition of ERK (U0126) and Akt (MK-2206) in P30 vascular smooth muscle cells (Fig. 5, I and J). These results suggested that G protein–dependent hypertrophic signaling was enhanced in P30 vascular smooth muscle cells. Egr-1 and platelet-derived growth factor–B (PDGF-B) are involved in the proliferative response to Ang II (*4*, *44*). We found that *Egr-1* induction by Ang II stimulation was enhanced in E17 neonatal vascular smooth muscle cells (Fig. 5K). The Ang II–induced increases in the expression of *Egr-1* and *PDGF-B* mRNA and DNA synthesis (as assessed by [^{3}H]thymidine incorporation) were significantly suppressed by U0126, but not by MK-2206 (Fig. 5, L to N). These results suggested that βArr-dependent activation of ERK was required for proliferative responses to Ang II.

Finally, we examined whether age-dependent changes in P2Y$_6$R abundance determine the balance of G protein–dependent hypertrophic and βArr-dependent proliferative responses by Ang II. Consistent with inhibition of the intracellular Ca^{2+} response (Fig. 2C), Ang II–induced increases in protein synthesis and cell size were significantly suppressed in *P2Y$_6$R*$^{(-/-)}$ vascular smooth muscle cells (Fig. 6A and fig. S8). Ang II–induced activation of p70S6K was also reduced in aortae from *P2Y$_6$R*$^{(-/-)}$ mice compared with those from *P2Y$_6$R*$^{(+/+)}$ mice (Fig. 6B and fig. S9). Ang II induced an increase in DNA synthesis in *P2Y$_6$R*$^{(-/-)}$, but not *P2Y$_6$R*$^{(+/+)}$, vascular

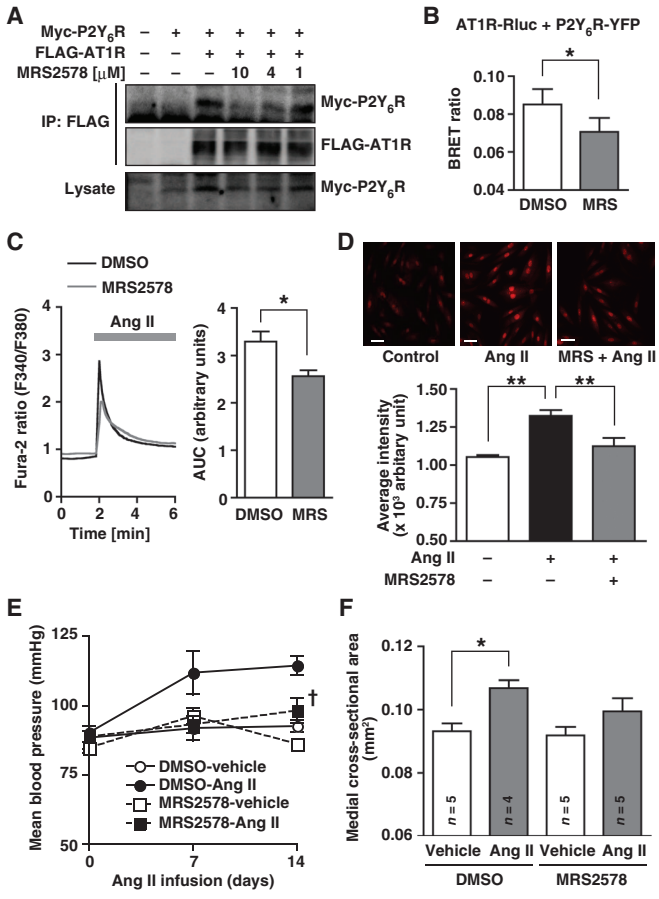

Fig. 4. MRS2578 inhibits Ang II–induced hypertension by disrupting AT1R-P2Y$_6$R heterodimer formation. (**A**) Effect of MRS2578 on the interaction of myc-P2Y$_6$R with FLAG-AT1R in VSMCs [n = 3 independent experiments; VSMCs were isolated from three *P2Y$_6$R*$^{(+/+)}$ mice]. (**B**) BRET ratio of VSMCs expressing AT1R-Rluc and P2Y$_6$R-YFP in the absence [dimethyl sulfoxide (DMSO)] or presence of MRS2578 [n = 4 independent experiments; VSMCs were isolated from three *P2Y$_6$R*$^{(+/+)}$ mice]. *P < 0.05. (**C**) Average traces of Ca^{2+} responses in VSMCs induced by Ang II. Right panel: Area under the curve (AUC) of Ca^{2+} responses induced by Ang II (n = 5 independent experiments; VSMCs were isolated from three P30 rats). *P < 0.05. (**D**) Effect of MRS2578 on Ang II–induced ROS generation in VSMCs (n = 6 independent experiments; VSMCs were isolated from three P30 rats). **P < 0.01. Scale bars, 50 μm. (**E**) Mean blood pressure (MBP) of mice infused with Ang II or vehicle in the absence (DMSO) or presence of MRS2578 (n = 5 mice per treatment). †P < 0.05 compared to mice infused with Ang II. (**F**) Quantification of the medial cross-sectional area of descending aortae (n = 4 to 5 mice per treatment). *P < 0.05.

smooth muscle cells (Fig. 6C). S II–induced ERK activation was enhanced in *P2Y$_6$R*$^{(-/-)}$ vascular smooth muscle cells (fig. S10A), suggesting that βArr-dependent proliferative signaling predominated in *P2Y$_6$R*$^{(-/-)}$ vascular smooth muscle cells. However, the number of medial nuclei was unchanged in descending aortae from Ang II–infused *P2Y$_6$R*$^{(-/-)}$ mice (fig. S10B). Therefore, proliferation of vascular smooth muscle cells in the aorta was strictly regulated in vivo. MRS2578 treatment inhibited Ang II–induced Akt activation and hypertrophic growth in P30 adult vascular smooth muscle cells (Fig. 6, D and E), which suggested a requirement for AT1R-P2Y$_6$R heterodimer formation in Ang II–induced vascular hypertrophy. In addition to the G$_q$-dependent hypertrophic response, MRS2578 inhibited Ang II–induced activation of RhoA, which mediates Gα$_{12/13}$-dependent procontractile signaling (fig. S11). In contrast, P2Y$_6$R overexpression in E17 neonatal vascular smooth muscle cells completely suppressed the Ang II–induced increases in *PDGF-B* mRNA expression and DNA synthesis (Fig. 6, F and G). In addition, P2Y$_6$R-overexpressed E17 cells showed increased hypertrophic signaling, including activation of p70S6K, Akt, and ERK (Fig. 6H) and enhanced basal protein synthesis (Fig. 6I). Furthermore, *P2Y$_6$R* mRNA was greater in the descending aorta of older mice compared with that of young adult mice (Fig. 6J). These results support the idea that the increase in P2Y$_6$R abundance that occurs with age converts AT1R-stimulated signaling in vascular smooth muscle cells from βArr-dependent proliferation to G protein–dependent hypertrophy (Fig. 6K).

DISCUSSION

We found that P2Y$_6$R promoted Ang II–triggered hypertrophic signals in vascular smooth muscle cells (Fig. 6). Accordingly, P2Y$_6$R deletion attenuated Ang II–induced hypertension and vascular remodeling in mice (Fig. 1). Heterodimer formation between AT1R and P2Y$_6$R played an important role in P2Y$_6$R-mediated regulation of Ang II responses (Fig. 4). Several GPCRs have been identified as the dimerization partners of AT1R (*17*). Tissue-specific regulation of Ang II signaling may explain why AT1R can form a heterodimer with various GPCRs. The α_{2C}-adrenergic receptor–AT1R complex is involved in norepinephrine secretion in sympathetic neurons (*22*), and the cannabinoid CB$_1$R-AT1R complex acts in activated hepatic stellate cells (*18*). The bradykinin B2R-AT1R heterodimer is abundant in omental vessels from preeclamptic women (*45*) and mesangial cells from hypertensive rats (*46*). Our study showed that the AT1R-P2Y$_6$R complex regulated Ang II–evoked vascular remodeling in the thoracic aorta and supports the notion that heterodimerization of AT1R may generate functional diversity of Ang II responses in different tissues and under different conditions.

AT1R can associate with various GPCRs. Identification of the molecular mechanism of heterodimerization of AT1R and P2Y$_6$R could lead to understanding of the mechanism underlying heterodimerization of GPCRs. In our study, the P2Y$_6$R antagonist MRS2578 inhibited the interaction of both receptors (Fig. 4), whereas the P2Y$_6$R selective agonist 3-pUDP and the AT1R antagonist losartan did not affect this interaction (fig. S2). These findings suggested that the MRS2578-induced conformational change of P2Y$_6$R is critical for AT1R interaction. Future structural biological analysis focusing on the conformational change of P2Y$_6$R induced by MRS2578 may help to understand the molecular basis of AT1R-P2Y$_6$R heterodimerization.

Mass spectrometry analysis has shown that the concentration of Ang II in human plasma is about 20 pM in healthy subjects and about 70 pM in chronic kidney disease patients (*47*). Although locally generated Ang II may increase local Ang II concentrations, which act on vascular smooth muscle cells, the Ang II concentrations that we used in this study, especially in vitro, would be too high. Therefore, an aberrant increase in plasma Ang II concentrations under pathophysiological conditions may be required to induce AT1R-mediated hypertensive signaling in vivo. An alternative possibility is the activation of AT1R by mechanical stress in an Ang II–independent manner (*48*). Thus, both chemical and physical stimulation may cooperatively activate AT1R-P2Y$_6$R heterodimer to induce hypertension, although it is not known whether AT1R-P2Y$_6$R heterodimer responds to mechanical stretch.

Ang II triggers hypertrophic and hyperplastic responses of vascular smooth muscle cells. In our study, Ang II induced βArr-dependent proliferative and G protein–dependent hypertrophic responses in neonatal and adult

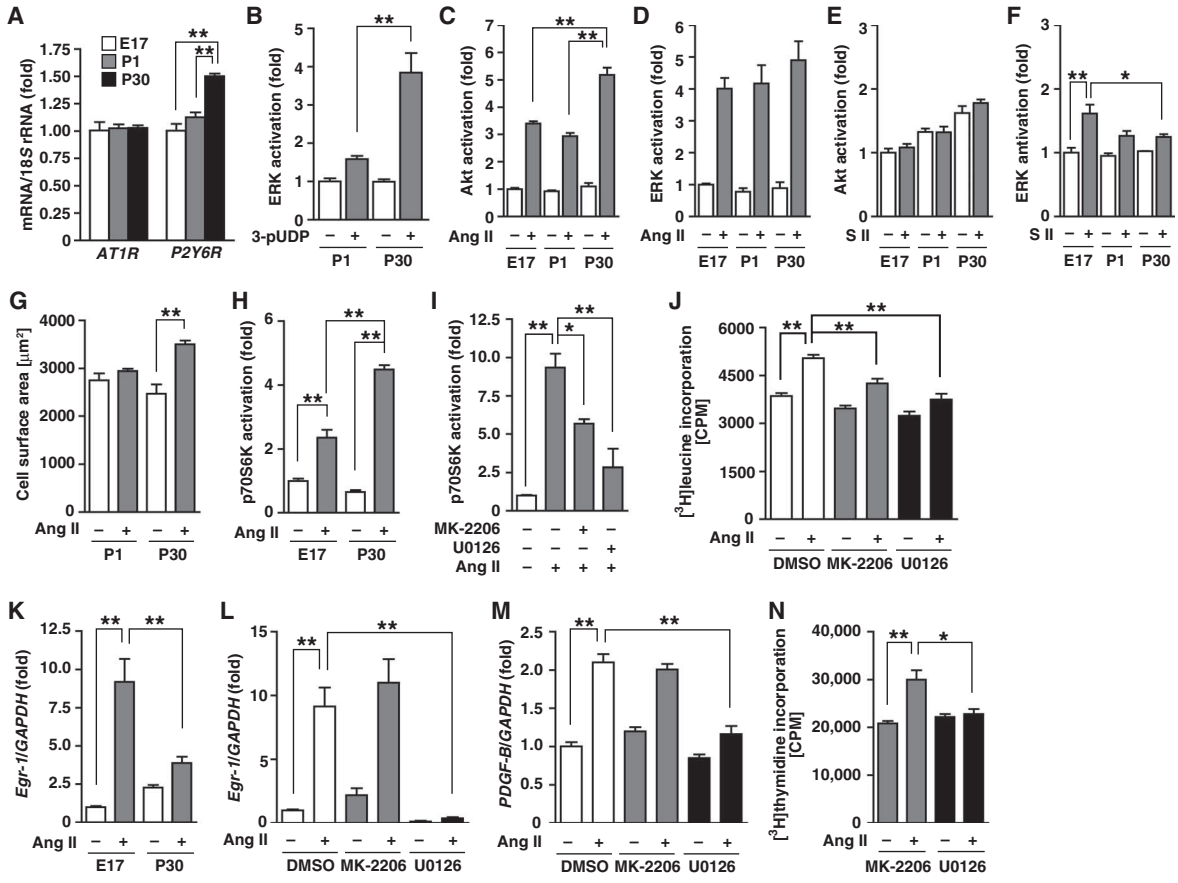

Fig. 5. Ang II induces hyperplastic or hypertrophic signaling in VSMCs depending on the developmental stage. (A) Expression of mRNAs for *AT1R* and *P2Y$_6$R* in VSMCs from E17, P1, or P30 rats (n = 3 biological replicates; VSMCs were isolated from 10 E17, 10 P1, and 3 P30 rats). $^{**}P < 0.01$. (B) ERK activation of P1 and P30 VSMCs induced by 3-pUDP (n = 3 independent experiments; VSMCs were isolated from 10 P1 and 3 P30 rats). $^{**}P < 0.01$. (C to F) ERK and Akt activation of E17, P1, or P30 VSMCs exposed to Ang II (C and D) or S II (E and F) (n = 3 independent experiments; VSMCs were isolated from 10 E17, 10 P1, and 3 P30 rats). $^{*}P < 0.05$, $^{**}P < 0.01$. (G) Hypertrophic growth of P1 and P30 VSMCs induced by Ang II (n = 3 independent experiments; VSMCs were isolated from 10 P1 and 3 P30 rats). $^{**}P < 0.01$. (H) p70S6K activation of E17 and P30 VSMCs exposed to Ang II (n = 3 independent experiments; VSMCs were isolated from 10 E17 and 3 P30 rats). $^{**}P < 0.01$. (I and J) Effects of MK-2206 and U0126 on p70S6K activation (I) and [^{3}H]leucine incorporation (J) in P30 VSMCs exposed to Ang II [n = 3 (I) or n = 4 (J) independent experiments; VSMCs were isolated from three P30 rats]. $^{*}P < 0.05$, $^{**}P < 0.01$. CPM, counts per minute. (K) Expression of *Egr-1* mRNA in E17 and P30 VSMCs exposed to Ang II (n = 3 biological replicates; VSMCs were isolated from 10 E17 and 3 P30 rats). $^{**}P < 0.01$. (L to N) Effects of MK-2206 and U0126 on mRNA expression of *Egr-1* (L) and *PDGF-B* (M) and [^{3}H] thymidine incorporation (N) in E17 VSMCs exposed to Ang II (n = 3 biological replicates; VSMCs were isolated from 10 E17 rats). $^{*}P < 0.05$, $^{**}P < 0.01$.

vascular smooth muscle cells, respectively (Fig. 5). This finding is consistent with a previous report that Ang II stimulates PDGF-B abundance and promotes DNA synthesis in newborn, but not adult, vascular smooth muscle cells (*4*). We found that the age-dependent changes in P2Y$_6$R abundance determined the balance of hypertrophic and hyperplastic signaling induced by Ang II (Fig. 6). Increased P2Y$_6$R abundance in adult vascular smooth muscle cells inhibited Ang II–induced recruitment of βArr to AT1R and receptor desensitization (Fig. 3), suggesting preferential activation of G protein–dependent signaling. G$_q$ protein–dependent activation of Akt mediated Ang II–induced hypertrophic signaling, whereas Ang II–induced ERK contributed to hypertrophic and proliferative signals (Fig. 5, J and N). Our results suggested that these two G$_q$ effectors differentially regulated the Ang II–induced responses in vascular smooth muscle cells as follows. G protein–dependent activation of ERK and Akt stimulated p70S6K, a major regulator of hypertrophic growth (*43*), and βArr-dependent ERK increased expression of *Egr-1* through Elk-1, a nuclear regulator of cell proliferation (*44*). The proliferative phenotype of vascular smooth muscle cells during neointimal formation relies on the ERK/Elk-1/Egr-1 pathway (*44*). We found that βArr-dependent ERK activation mediated the Ang II–induced Elk-1/Egr-1 axis in the nucleus (Fig. 5). Our results are supported by a previous report that μ-opioid receptor activation by morphine leads to cytosolic ERK activation through a G protein–dependent pathway, whereas etorphine induces nuclear ERK activation through a βArr-dependent manner (*49*). Additionally, in cardiomyocytes, Ang II–evoked ERK activation through the βArr2-dependent pathway supports proliferation, whereas G protein–mediated ERK activity induces hypertrophy (*50*).

In addition to developmentally induced changes in abundance, P2Y$_6$R abundance is also increased in pathological conditions. Inflammation reportedly increases P2Y$_6$R abundance in endothelial and epithelial cells (*36*, *51*). We have previously shown that pressure overload and constitutive

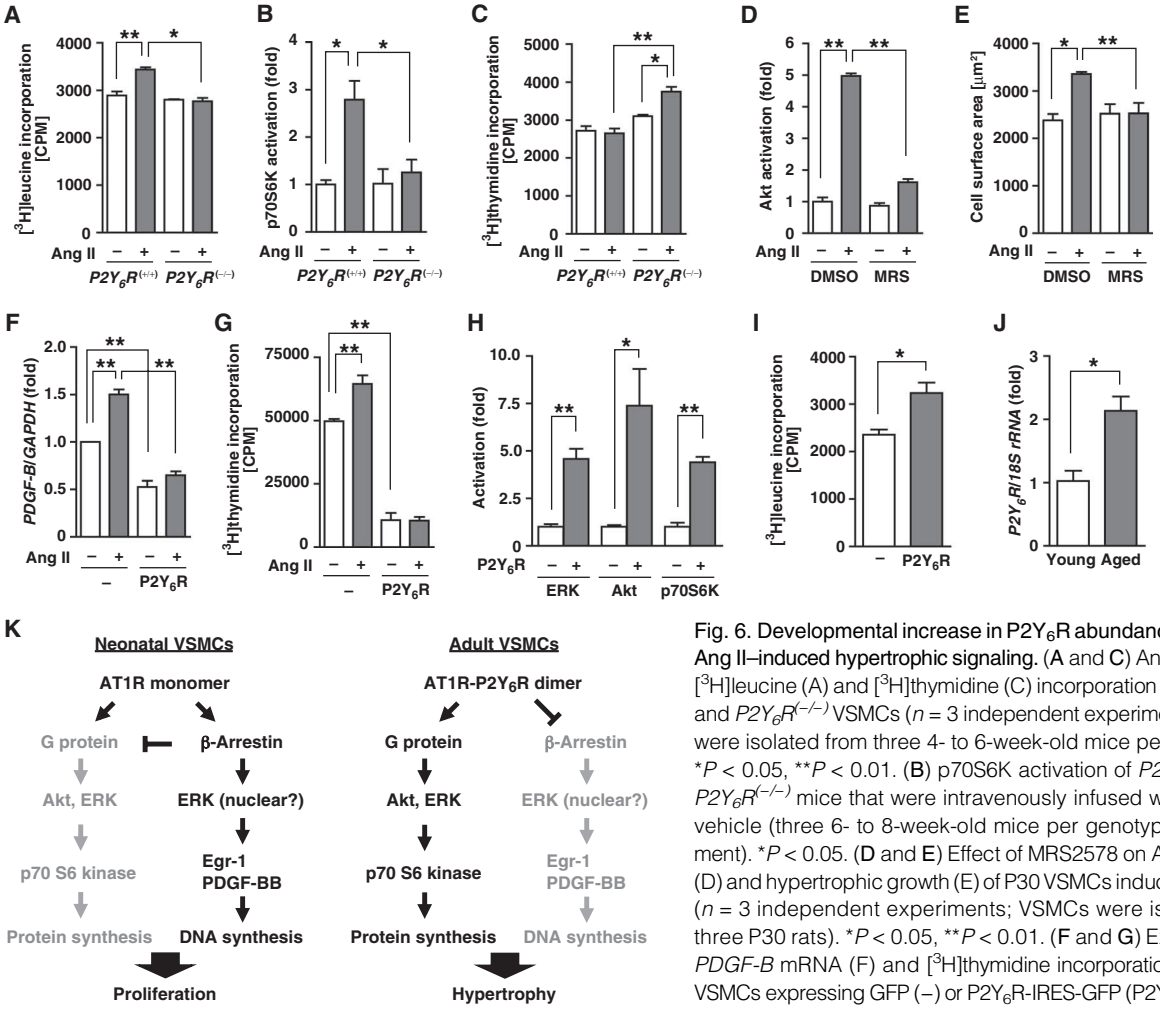

Fig. 6. Developmental increase in $P2Y_6R$ abundance enhances Ang II–induced hypertrophic signaling. (**A** and **C**) Ang II–induced [^{3}H]leucine (A) and [^{3}H]thymidine (C) incorporation in $P2Y_6R^{(+/+)}$ and $P2Y_6R^{(-/-)}$ VSMCs ($n = 3$ independent experiments; VSMCs were isolated from three 4- to 6-week-old mice per genotype). $^*P < 0.05$, $^{**}P < 0.01$. (**B**) p70S6K activation of $P2Y_6R^{(+/+)}$ and $P2Y_6R^{(-/-)}$ mice that were intravenously infused with Ang II or vehicle (three 6- to 8-week-old mice per genotype and treatment). $^*P < 0.05$. (**D** and **E**) Effect of MRS2578 on Akt activation (D) and hypertrophic growth (E) of P30 VSMCs induced by Ang II ($n = 3$ independent experiments; VSMCs were isolated from three P30 rats). $^*P < 0.05$, $^{**}P < 0.01$. (**F** and **G**) Expression of *PDGF-B* mRNA (F) and [^{3}H]thymidine incorporation (G) in E17 VSMCs expressing GFP (–) or $P2Y_6R$-IRES-GFP ($P2Y_6R$) induced by Ang II ($n = 3$ biological replicates; VSMCs were isolated from 10 E17 rats). $^{**}P < 0.01$. (**H** and **I**) Activation of ERK, Akt, and p70S6K (H) and [^{3}H]leucine incorporation (I) in E17 VSMCs expressing GFP (–) or $P2Y_6R$-IRES-GFP ($P2Y_6R$) ($n = 3$ independent experiments; VSMCs were isolated from 10 E17 rats). $^*P < 0.05$, $^{**}P < 0.01$. (**J**) Expression of $P2Y_6R$ mRNA in descending aortae isolated from young adult (12 weeks) or aged (1 year) mice ($n = 3$ mice per developmental stage). $^*P < 0.05$. (**K**) Working model for Ang II–induced signaling in neonatal (low $P2Y_6R$ abundance) and adult (high $P2Y_6R$ abundance) VSMCs.

activation of $G\alpha_{13}$ increase $P2Y_6R$ abundance in mouse hearts (*38*). We also found that $P2Y_6R$ abundance was increased in the descending aorta of older mice (Fig. 6J). This evidence suggests that environmental risk factors, including inflammation, mechanical stress, and aging, raise the probability of hypertension through increases in $P2Y_6R$ abundance.

We also found that the $P2Y_6R$-specific antagonist MRS2578 (*41*) disrupted the interaction of AT1R and $P2Y_6R$ (Fig. 4, A and B), and infusion of MRS2578 reduced Ang II–induced hypertension and vascular hypertrophy in mice (Fig. 4, E and F). This experimental evidence suggests that AT1R-$P2Y_6R$ heterodimerization could be a potential therapeutic target for hypertension. Although angiotensin-converting enzyme inhibitors and angiotensin receptor blockers are widely used in the treatment of hypertension, they increase the risk for congenital anomalies in infants if women take these medicines during pregnancy (*52*). Genetic mutations in genes encoding the renin-angiotensin system have been identified in patients who have renal tubular dysgenesis (*53*). Additionally, mice lacking renin-angiotensin system genes have abnormal renal development (*54*), whereas $P2Y_6R$ knockout mice show normal kidney development (*35*). Therefore, compounds that disrupt the AT1R-$P2Y_6R$ heterodimer might be attractive drug candidates to treat hypertension without triggering abnormalities in kidney development.

MATERIALS AND METHODS

Materials

Ang II was purchased from Peptide Institute. Paraformaldehyde (PFA) and 10% formalin neutral buffer solution were from Wako. Dihydroethidium (DHE), UDP, and MRS2578 were from Sigma. 3-pUDP (PSB 0474) was from Tocris. Fura-2 AM was from Dojindo. [^{3}H]Leucine (NET135H) and [^{3}H]thymidine (NET027E) were from PerkinElmer. The following antibodies were purchased: anti-FLAG M2 horseradish peroxidase–conjugated and anti–α–smooth muscle actin (αSMA) (Sigma); anti–4-HNE (Japan Institute for the Control of Aging); anti-GFP and anti–SM-MHC11 (Abcam); anti-myc (Millipore); anti–phospho-Akt (#4060), anti-Akt, anti–phospho-ERK

(#4370), anti-ERK, anti–phospho-p70S6K (#9204), and anti-p70S6K (Cell Signaling Technology).

Experimental animals

Animal care and handling were carried out according to guidelines approved by the Animal Care and Use Ethical Committee of Kyushu University and the ethic committees at the National Institute for Physiological Sciences. Rodents were housed in air-conditioned conventional rooms with time-controlled lighting system. $P2Y_6R^{(-/-)}$ mice were backcrossed onto a C57BL/6 background to obtain $P2Y_6R$ heterozygotes [$P2Y_6R^{(+/-)}$]. Six- to 8-week-old male mice were used for experiments. Briefly, rodents were anesthetized by an intraperitoneal injection of midazolam (4 mg/kg), medetomidine hydrochloride (0.3 mg/kg), and butorphanol (5 mg/kg). A mini-osmotic pump (ALZET) filled with vehicle [phosphate buffered saline (PBS)] or Ang II (2 mg/kg per day) was intraperitoneally implanted into mice, and Ang II or PBS was continuously administered for 4 weeks. For acute infusion, mice were anesthetized and then Ang II (10 μM, 30 μl) was injected into the jugular vein. After 10 min, thoracic aortae were isolated.

Measurement of blood pressure and heart rate

Systolic blood pressure, diastolic blood pressure, MBP, and heart rate in the daytime (2:00 p.m. to 5:00 p.m.) were measured in conscious mice using a noninvasive computerized tail-cuff system (BP-98AW, Softron). An average of 10 consecutive measurements per mouse was taken.

Histological analysis

Mice were sacrificed by intraperitoneal injection of midazolam, medetomidine hydrochloride, and butorphanol. The descending thoracic aorta was carefully isolated and cleaned of any adhering connective tissue. Paraffin-embedded specimens were stained with H&E. Digital images were obtained using ECLIPSE 80i (Nikon). The H&E-stained medial cross-sectional areas, wall-to-lumen ratio, and number of nuclei were measured by ImageJ software. Fibrotic tissues were stained using Picrosirius red staining. Specimens embedded in OCT (optimum cutting temperature) compound were used to analyze ROS formation. Aortae were stained with anti–4-HNE antibody. The 4-HNE adducts were detected with Alexa Fluor 546 anti-mouse immunoglobulin G antibody. Digital images were taken at ×60 magnification using confocal microscopy (FV10i, Olympus), and five regions were randomly selected for each specimen. The average intensity was analyzed using MetaMorph software (Molecular Devices).

Measurement of vascular contraction and endothelial-dependent relaxation

Isometric tension was measured as previously described (*55*). To analyze endothelium-dependent relaxation, abdominal aortae were carefully isolated from $P2Y_6R^{(+/+)}$ or $P2Y_6R^{(-/-)}$ mice that were infused with or without Ang II. The aortic rings were precontracted with norepinephrine (1 mM), and endothelial function was determined by examining the degree of relaxation in response to UDP. To measure vascular contraction, aortic rings were contracted with 100 mM KCl before measurement of Ang II–induced vascular contraction. The magnitude of the response was shown as a percentage of the reference constriction in response to 100 mM KCl.

Measurement of UDP concentration in mouse plasma

The blood samples were centrifuged at 2000*g* for 5 min and subsequently at 9000*g* for 5 min to isolate plasma. Collected plasma was then mixed with phenol/chloroform/isoamyl alcohol (25:24:1, v/v, pH 7.9; Nacalai Tesque Inc.), and after brief vortex, samples were centrifuged for 2 hours at 4°C. The aqueous phase was collected and washed three times with diethyl ether. All samples were filtered by Ultrafree-MC (Amicon) before high-performance liquid chromatography (HPLC) analysis. The concentration of nucleotides in the serum was analyzed using an HPLC system (Jasco) with an octadecylsilyl column (4.6 × 150 mm; GL Sciences Inc.) as previously described (*56*). The mobile phase consisted of 8 mM tetrabutylammonium hydrogen sulfate (TBAHS), 35 mM KH_2PO_4, 15% MeOH (pH 3.5; solvent A), and 8 mM TBAHS, 35 mM KH_2PO_4, 50% methanol (pH 2.8; solvent B). The mobile phase was developed at 0.8 ml/min from 0 to 15 min in 100% solvent A, and from 15 to 30 min in 50% solvent B. Absorbance at 260 nm was monitored online with an UV-2075 UV (ultraviolet) detector (Jasco).

Cell culture

Primary mouse vascular smooth muscle cells were isolated by the enzymatic dispersion method. Thoracic aortae from three 4- to 6-week-old mice were quickly isolated, and perivascular fat and adventitia were discarded. Vessels were cut into small pieces and then digested by collagenase II and elastase at 37°C for 1 hour. The isolated cells were plated in Dulbecco's modified Eagle's medium (DMEM)/F-12 containing 20% fetal bovine serum (FBS). Primary rat vascular smooth muscle cells were isolated from 10 E17, 10 P1, or 3 P30 rat thoracic aortae, and cultured in low-glucose DMEM containing 10% FBS. HEK293 cells were cultured in high-glucose DMEM containing 10% FBS. Plasmid DNA was transfected into HEK293 cells or smooth muscle cells using X-tremeGENE 9 (Roche) or ViaFect (Promega), respectively.

Infection of recombinant adenoviruses

Recombinant adenoviruses expressing G protein inhibitory peptide ($G\alpha_s$ct, $G\alpha_i$ct, $G\alpha_q$ct, or p115RGS) were generated and amplified as previously described (*57*). Vascular smooth muscle cells were infected with recombinant adenoviruses at a multiplicity of infection of 50 for 24 hours. Cells were then starved in serum-free medium and cultured for an additional 24 hours. Under these conditions, almost 80% of cells were GFP-positive.

Intracellular Ca^{2+} imaging

Intracellular Ca^{2+} was measured using Fura-2 as previously described (*8*). For the $P2Y_6R$ rescue experiment, vascular smooth muscle cells from $P2Y_6R^{(-/-)}$ mice were infected with retrovirus encoding IRES-GFP or $P2Y_6R$-IRES-GFP, and images of Fura-2 fluorescence of GFP-positive cells were analyzed.

Immunoprecipitation

HEK293 cells transfected with myc-$P2Y_6R$ and FLAG-AT1R were lysed in lysis buffer A [20 mM Hepes (pH 7.4), 100 mM NaCl, 3 mM $MgCl_2$, and 1% NP-40] containing protease inhibitor cocktail for 15 min at 4°C. Cleared lysates were immunoprecipitated with anti-FLAG M2 agarose beads (Sigma) for 2 hours. Agonist-induced interaction between FLAG-AT1R and βArr2-YFP was detected by cross-linking experiments. In brief, transfected HEK293 cells were treated with 100 nM Ang II for 10 min. After washing with PBS, cells were incubated with 2 mM dithiobis(succinimidyl propionate) (DSP) cross-linker for 30 min at room temperature. The cross-linking reaction was quenched by the addition of tris-HCl (pH 7.5) at a final concentration of 50 mM. After washing twice with PBS, cells were lysed and immunoprecipitated. For inhibitor treatment, transfected vascular smooth muscle cells were treated with indicated concentrations of MRS2578 for 30 min and then lysed.

Small interfering RNA transfection

Vascular smooth muscle cells were transfected with small interfering RNAs (siRNAs) (20 nM) using Lipofectamine RNAiMAX reagent (Life Technologies). The siRNA sequences used in this study are listed in table S1. The

gene silencing of mouse βArr1, mouse βArr2, rat βArr1, or rat βArr2 mRNA were 86 ± 6%, 49 ± 3%, 86 ± 6%, or 75 ± 1%, respectively (n = 3 biological replicates). Silencing efficiency was assessed by quantitative real-time polymerase chain reaction (PCR).

RNA preparation and real-time PCR

Total RNA was purified from cultured cells using Qiagen RNeasy Mini Kit. Real-time PCR was performed using Power SYBR Green PCR Master Mix (Life Technologies) or QuantiTect Probe RT-PCR Kit (Qiagen) and TaqMan probes. TaqMan probe and primer sequences are listed in table S2. Expression was normalized to 18*S* ribosomal RNA or *GAPDH* as the internal control.

Immunofluorescence

Transfected HEK293 cells were seeded on poly-L-lysine–coated glass-bottom dish and stimulated with 100 nM Ang II for 15 min. To assess hypertrophy, vascular smooth muscle cells were seeded on glass-bottom dish at 4×10^4 cells per dish and serum-starved for 48 hours. Cells were then stimulated with 100 nM Ang II for 1 to 3 days. After stimulation, cells were fixed with 4% PFA for 15 min and permeabilized with 0.2 saponin or 0.1% Triton X-100 for 5 min. After washing with PBS, cells were incubated with blocking buffer (10% FBS in PBS) for 1 hour. Cells were stained with primary antibodies for FLAG, myc, αSMA, or SM-MHC11 at 4°C overnight. After washing with PBS, cells were incubated with CF488- or CF594-conjugated secondary antibodies (Biotium) for 1 hour. After washing with PBS, cells were incubated with DAPI (4′,6-diamidino-2-phenylindole) and then imaged on a confocal microscope (FV10i, Olympus). Cell surface area was quantified from more than 30 cells at each condition using FV10-ASW software.

Western blotting

Serum-starved vascular smooth muscle cells were pretreated with 10 μM MRS2578, 5 μM MK-2206, or 5 μM U0126 for 30 min, then stimulated with 100 nM Ang II, 10 μM S II, or 1 μM 3-pUDP for 5 min, and then harvested with lysis buffer B (lysis buffer A with 50 mM NaF, 1 mM Na_3VO_4, and 20 mM β-glycerophosphate) containing protease inhibitor cocktail for 15 min at 4°C. Cleared lysates were mixed with sample buffer.

RhoA activation

Vascular smooth muscle cells were plated on six-well plates at 1.5×10^5 cells per well. After 24 hours, cells were starved in serum-free medium for another 24 hours. Cells were pretreated with 10 μM MRS2578 for 25 min and then stimulated with 100 nM Ang II for 5 min. RhoA activation was measured by G-LISA RhoA Activation Kit (Cytoskeleton) according to the manufacturer's protocol.

[^{3}H]Leucine and [^{3}H]thymidine incorporation

Vascular smooth muscle cells were plated on 24-well plates at 3×10^4 cells per well. After 24 hours, cells were starved in serum-free medium for another 24 hours. Cells were pretreated with 1 μM MRS2578, 3 μM MK2206, or 3 μM U0126 for 30 min, and then incubated with 100 nM Ang II together with [^{3}H]leucine or [^{3}H]thymidine (1 μCi/ml) for an additional 24 hours. Cells were washed with ice-cold PBS and fixed in 10% trichloroacetic acid. Cells were lysed in 0.4 N NaOH, and incorporated [^{3}H]leucine or [^{3}H]thymidine was measured by a liquid scintillation counter. To discriminate hypertrophy from proliferation in cell culture, values of [^{3}H]leucine were normalized to DNA content determined by QuantiFluor dsDNA System (Promega).

Measurement of ROS

Vascular smooth muscle cells were plated on 35-mm glass-bottom dish at 1×10^5 cells per dish. ROS production was detected by loading DHE (10 μM) at 37°C for 10 min before Ang II administration. The DHE fluorescence was observed using FV10i confocal microscope at 543-nm excitation and 560-nm emission wavelength, and DHE fluorescence intensity was quantified using FV10-ASW software.

Bioluminescence resonance energy transfer

HEK293 cells or vascular smooth muscle cells were seeded on a 12- or 6-well plate, respectively, 24 hours before transfection. To analyze the interaction of AT1R and $P2Y_6R$, BRET between AT1R-Rluc (donor) and $P2Y_6R$-YFP (acceptor) was measured. For the BRET saturation assay, HEK293 cells were transfected with a constant amount of AT1R-Rluc with an increasing amount of $P2Y_6R$-YFP or YFP as a negative control. For the BRET competition assay, HEK293 cells were transfected with a constant amount of AT1R-Rluc and $P2Y_6R$-YFP with an increasing amount of FLAG-$P2Y_6R$ as a competitor. For the βArr recruitment assay, AT1R-Rluc was transfected alone or with βArr2-YFP. To evaluate colocalization of AT1R with membrane compartment markers, AT1R-Rluc was transfected alone or with Venus-PM (C-terminal peptide of K-Ras, plasma membrane). After 48 hours of transfection, cells were suspended in PBS containing $CaCl_2$, $MgCl_2$, and glucose, and were transferred to 96-well plates. Coelenterazine h (5 μM) and 100 nM Ang II were added 10 min before BRET measurement. Luminescence and fluorescence signals were detected using SpectraMax i3 (Molecular Devices). The BRET ratio was calculated by dividing the fluorescence signal (531/22 emission filter) by the luminescence signal (485/20 emission filters).

Statistical analysis

Results are represented as means ± SEM. All experiments were repeated at least three times. For a normal distribution, statistical significance was determined by unpaired t test for two-group comparison and by one-way analysis of variance with Tukey's post hoc test for comparison among three or more groups. For a nonnormal distribution, statistical significance was determined by the Mann-Whitney test for two-group comparison and by the Kruskal-Wallis test with Dunn's post hoc test for comparison among three or more groups. Significance was considered at $P < 0.05$.

SUPPLEMENTARY MATERIALS

www.sciencesignaling.org/cgi/content/full/9/411/ra7/DC1

Fig. S1. Involvement of βArr2 in Ang II–induced AT1R internalization.
Fig. S2. Effects of agonists and antagonists on the heterodimerization of AT1R and $P2Y_6R$.
Fig. S3. $P2Y_6R$ activation by Up_4A.
Fig. S4. Ang II–induced activation of various signaling pathways in VSMCs from different developmental stages.
Fig. S5. Ang II induces Akt activation through G_q in VSMCs.
Fig. S6. Involvement of βArr in Ang II–mediated hyperplastic and hypertrophic signaling in VSMCs.
Fig. S7. Ang II promotes contractile differentiation of adult VSMCs.
Fig. S8. *P2Y$_6$R* deletion inhibits Ang II–induced hypertrophic growth.
Fig. S9. Developmental increases in $P2Y_6R$ abundance enhance Ang II–induced hypertrophic signaling.
Fig. S10. *P2Y$_6$R* deletion potentiates βArr-dependent signaling.
Fig. S11. MRS2578 attenuates Ang II–induced RhoA activation.
Table S1. List of siRNAs.
Table S2. List of Taqman probe and primer sets for real-time PCR.

REFERENCES AND NOTES

1. A. Daugherty, L. Cassis, Angiotensin II-mediated development of vascular diseases. *Trends Cardiovasc. Med.* **14**, 117–120 (2004).
2. S. Heeneman, J. C. Sluimer, M. J. A. P. Daemen, Angiotensin-converting enzyme and vascular remodeling. *Circ. Res.* **101**, 441–454 (2007).
3. K. Ohtani, K. Egashira, Y. Ihara, K. Nakano, K. Funakoshi, G. Zhao, M. Sata, K. Sunagawa, Angiotensin II type 1 receptor blockade attenuates in-stent restenosis by inhibiting inflammation and progenitor cells. *Hypertension* **48**, 664–670 (2006).

4. J. Deguchi, M. Makuuchi, T. Nakaoka, T. Collins, Y. Takuwa, Angiotensin II stimulates platelet-derived growth factor-B chain expression in newborn rat vascular smooth muscle cells and neointimal cells through Ras, extracellular signal–regulated protein kinase, and c-Jun N-terminal protein kinase mechanisms. *Circ. Res.* **85**, 565–574 (1999).
5. G. Cai, H. Gurdal, T. M. Seasholtz, M. D. Johnson, Age-related changes in angiotensin II-stimulated vascular contraction and inositol phosphate accumulation in Fischer 344 rats. *Mech. Ageing Dev.* **76**, 125–133 (1994).
6. Z. Vamos, P. Cseplo, I. Ivic, R. Matics, J. Hamar, A. Koller, Age determines the magnitudes of angiotensin II-induced contractions, mRNA, and protein expression of angiotensin type 1 receptors in rat carotid arteries. *J. Gerontol. A Biol. Sci. Med. Sci.* **69**, 519–526 (2014).
7. B. C. Berk, Angiotensin type 2 receptor (AT2R): A challenging twin. *Sci. STKE* **2003**, PE16 (2003).
8. M. Nishida, S. Tanabe, Y. Maruyama, S. Mangmool, K. Urayama, Y. Nagamatsu, S. Takagahara, J. H. Turner, T. Kozasa, H. Kobayashi, Y. Sato, T. Kawanishi, R. Inoue, T. Nagao, H. Kurose, Gα12/13- and reactive oxygen species-dependent activation of c-Jun NH_2-terminal kinase and p38 mitogen-activated protein kinase by angiotensin receptor stimulation in rat neonatal cardiomyocytes. *J. Biol. Chem.* **280**, 18434–18441 (2005).
9. C. Guilluy, J. Brégeon, G. Toumaniantz, M. Rolli-Derkinderen, K. Retailleau, L. Loufrani, D. Henrion, E. Scalbert, A. Bril, R. M. Torres, S. Offermanns, P. Pacaud, G. Loirand, The Rho exchange factor Arhgef1 mediates the effects of angiotensin II on vascular tone and blood pressure. *Nat. Med.* **16**, 183–190 (2010).
10. S. M. DeWire, S. Ahn, R. J. Lefkowitz, S. K. Shenoy, β-Arrestins and cell signaling. *Annu. Rev. Physiol.* **69**, 483–510 (2007).
11. E. Reiter, R. J. Lefkowitz, GRKs and β-arrestins: Roles in receptor silencing, trafficking and signaling. *Trends Endocrinol. Metab.* **17**, 159–165 (2006).
12. T. Takahashi, T. Taniguchi, H. Konishi, U. Kikkawa, Y. Ishikawa, M. Yokoyama, Activation of Akt/protein kinase B after stimulation with angiotensin II in vascular smooth muscle cells. *Am. J. Physiol.* **276**, H1927–H1934 (1999).
13. P. K. Mehta, K. K. Griendling, Angiotensin II cell signaling: Physiological and pathological effects in the cardiovascular system. *Am. J. Physiol. Cell Physiol.* **292**, C82–C97 (2007).
14. M. R. Whorton, M. P. Bokoch, S. G. F. Rasmussen, B. Huang, R. N. Zare, B. Kobilka, R. K. Sunahara, A monomeric G protein-coupled receptor isolated in a high-density lipoprotein particle efficiently activates its G protein. *Proc. Natl. Acad. Sci. U.S.A.* **104**, 7682–7687 (2007).
15. O. P. Ernst, V. Gramse, M. Kolbe, K. P. Hofmann, M. Heck, Monomeric G protein-coupled receptor rhodopsin in solution activates its G protein transducin at the diffusion limit. *Proc. Natl. Acad. Sci. U.S.A.* **104**, 10859–10864 (2007).
16. S. Terrillon, M. Bouvier, Roles of G-protein-coupled receptor dimerization. *EMBO Rep.* **5**, 30–34 (2004).
17. S. AbdAlla, H. Lother, U. Quitterer, AT_1-receptor heterodimers show enhanced G-protein activation and altered receptor sequestration. *Nature* **407**, 94–98 (2000).
18. R. Rozenfeld, A. Gupta, K. Gagnidze, M. P. Lim, I. Gomes, D. Lee-Ramos, N. Nieto, L. A. Devi, AT1R–CB_1R heteromerization reveals a new mechanism for the pathogenic properties of angiotensin II. *EMBO J.* **30**, 2350–2363 (2011).
19. C. Zeng, Y. Luo, L. D. Asico, U. Hopfer, G. M. Eisner, R. A. Felder, P. A. Jose, Perturbation of D_1 dopamine and AT_1 receptor interaction in spontaneously hypertensive rats. *Hypertension* **42**, 787–792 (2003).
20. C. Zeng, L. D. Asico, X. Wang, U. Hopfer, G. M. Eisner, R. A. Felder, P. A. Jose, Angiotensin II regulation of AT_1 and D_3 dopamine receptors in renal proximal tubule cells of SHR. *Hypertension* **41**, 724–729 (2003).
21. M. de Lourdes González-Hernández, D. Godínez-Hernández, R. A. Bobadilla-Lugo, P. López-Sánchez, Angiotensin-II type 1 receptor (AT_1R) and alpha-1D adrenoceptor form a heterodimer during pregnancy-induced hypertension. *Auton. Autacoid Pharmacol.* **30**, 167–172 (2010).
22. M. Bellot, S. Galandrin, C. Boularan, H. J. Matthies, F. Despas, C. Denis, J. Javitch, S. Mazères, S. J. Sanni, V. Pons, M.-H. Seguelas, J. L. Hansen, A. Pathak, A. Galli, J.-M. Sénard, C. Galés, Dual agonist occupancy of AT_1-R–α_{2C}-AR heterodimers results in atypical G_s-PKA signaling. *Nat. Chem. Biol.* **11**, 271–279 (2015).
23. L. Barki-Harrington, L. M. Luttrell, H. A. Rockman, Dual inhibition of β-adrenergic and angiotensin II receptors by a single antagonist: A functional role for receptor–receptor interaction in vivo. *Circulation* **108**, 1611–1618 (2003).
24. M. Filizola, H. Weinstein, The study of G-protein coupled receptor oligomerization with computational modeling and bioinformatics. *FEBS J.* **272**, 2926–2938 (2005).
25. B. Szalai, L. Barkai, G. Turu, L. Szidonya, P. Várnai, L. Hunyady, Allosteric interactions within the AT_1 angiotensin receptor homodimer: Role of the conserved DRY motif. *Biochem. Pharmacol.* **84**, 477–485 (2012).
26. M. P. Abbracchio, G. Burnstock, J.-M. Boeynaems, E. A. Barnard, J. L. Boyer, C. Kennedy, G. E. Knight, M. Fumagalli, C. Gachet, K. A. Jacobson, G. A. Weisman, International Union of Pharmacology LVIII: Update on the P2Y G protein-coupled nucleotide receptors: From molecular mechanisms and pathophysiology to therapy. *Pharmacol. Rev.* **58**, 281–341 (2006).
27. G. Burnstock, Purine and pyrimidine receptors. *Cell. Mol. Life Sci.* **64**, 1471–1483 (2007).
28. E. R. Lazarowski, R. C. Boucher, T. K. Harden, Constitutive release of ATP and evidence for major contribution of ecto-nucleotide pyrophosphatase and nucleoside diphosphokinase to extracellular nucleotide concentrations. *J. Biol. Chem.* **275**, 31061–31068 (2000).
29. M. R. Elliott, F. B. Chekeni, P. C. Trampont, E. R. Lazarowski, A. Kadl, S. F. Walk, D. Park, R. I. Woodson, M. Ostankovich, P. Sharma, J. J. Lysiak, T. K. Harden, N. Leitinger, K. S. Ravichandran, Nucleotides released by apoptotic cells act as a find-me signal to promote phagocytic clearance. *Nature* **461**, 282–286 (2009).
30. V. Jankowski, M. Tölle, R. Vanholder, G. Schönfelder, M. van der Giet, L. Henning, H. Schlüter, M. Paul, W. Zidek, J. Jankowski, Uridine adenosine tetraphosphate: A novel endothelium-derived vasoconstrictive factor. *Nat. Med.* **11**, 223–227 (2005).
31. J. Jankowski, V. Jankowski, B. Seibt, L. Henning, W. Zidek, H. Schlüter, Identification of dinucleoside polyphosphates in adrenal glands. *Biochem. Biophys. Res. Commun.* **304**, 365–370 (2003).
32. T. Matsumoto, R. C. Tostes, R. C. Webb, The role of uridine adenosine tetraphosphate in the vascular system. *Adv. Pharmacol. Sci.* **2011**, 435132 (2011).
33. J. D. Pediani, J. C. McGrath, S. M. Wilson, P2Y receptor-mediated Ca^{2+} signalling in cultured rat aortic smooth muscle cells. *Br. J. Pharmacol.* **126**, 1660–1666 (1999).
34. L. Wang, L. Karlsson, S. Moses, A. Hultgårdh-Nilsson, M. Andersson, C. Borna, T. Gudbjartsson, S. Jern, D. Erlinge, P2 receptor expression profiles in human vascular smooth muscle and endothelial cells. *J. Cardiovasc. Pharmacol.* **40**, 841–853 (2002).
35. I. Bar, P.-J. Guns, J. Metallo, D. Cammarata, F. Wilkin, J.-M. Boeynams, H. Bult, B. Robaye, Knockout mice reveal a role for $P2Y_6$ receptor in macrophages, endothelial cells, and vascular smooth muscle cells. *Mol. Pharmacol.* **74**, 777–784 (2008).
36. A.-K. Riegel, M. Faigle, S. Zug, P. Rosenberger, B. Robaye, J.-M. Boeynaems, M. Idzko, H. K. Eltzschig, Selective induction of endothelial $P2Y_6$ nucleotide receptor promotes vascular inflammation. *Blood* **117**, 2548–2555 (2011).
37. P. Stachon, A. Peikert, N. A. Michel, S. Hergeth, T. Marchini, D. Wolf, B. Dufner, N. Hoppe, C. K. Ayata, M. Grimm, S. Cicko, L. Schulte, J. Reinöhl, C. von zur Muhlen, C. Bode, M. Idzko, A. Zirlik, $P2Y_6$ deficiency limits vascular inflammation and atherosclerosis in mice. *Arterioscler. Thromb. Vasc. Biol.* **34**, 2237–2245 (2014).
38. M. Nishida, Y. Sato, A. Uemura, Y. Narita, H. Tozaki-Saitoh, M. Nakaya, T. Ide, K. Suzuki, K. Inoue, T. Nagao, H. Kurose, $P2Y_6$ receptor-$G\alpha_{12/13}$ signalling in cardiomyocytes triggers pressure overload-induced cardiac fibrosis. *EMBO J.* **27**, 3104–3115 (2008).
39. K. Uchida, 4-Hydroxy-2-nonenal: A product and mediator of oxidative stress. *Prog. Lipid Res.* **42**, 318–343 (2003).
40. S. Buvinic, R. Briones, J. P. Huidobro-Toro, $P2Y_1$ and $P2Y_2$ receptors are coupled to the NO/cGMP pathway to vasodilate the rat arterial mesenteric bed. *Br. J. Pharmacol.* **136**, 847–856 (2002).
41. L. K. Mamedova, B. V. Joshi, Z.-G. Gao, I. von Kügelgen, K. A. Jacobson, Diisothiocyanate derivatives as potent, insurmountable antagonists of $P2Y_6$ nucleotide receptors. *Biochem. Pharmacol.* **67**, 1763–1770 (2004).
42. G. K. Owens, M. S. Kumar, B. R. Wamhoff, Molecular regulation of vascular smooth muscle cell differentiation in development and disease. *Physiol. Rev.* **84**, 767–801 (2004).
43. R. M. Touyz, E. L. Schiffrin, Signal transduction mechanisms mediating the physiological and pathophysiological actions of angiotensin II in vascular smooth muscle cells. *Pharmacol. Rev.* **52**, 639–672 (2000).
44. T. F. Althoff, J. Albarrán Juárez, K. Troidl, C. Tang, S. Wang, A. Wirth, M. Takefuji, N. Wettschureck, S. Offermanns, Procontractile G protein–mediated signaling pathways antagonistically regulate smooth muscle differentiation in vascular remodeling. *J. Exp. Med.* **209**, 2277–2290 (2012).
45. S. AbdAlla, H. Lother, A. el Massiery, U. Quitterer, Increased AT_1 receptor heterodimers in preeclampsia mediate enhanced angiotensin II responsiveness. *Nat. Med.* **7**, 1003–1009 (2001).
46. S. AbdAlla, A. Abdel-Baset, H. Lother, A. el Massiery, U. Quitterer, Mesangial AT_1/B_2 receptor heterodimers contribute to angiotensin II hyperresponsiveness in experimental hypertension. *J. Mol. Neurosci.* **26**, 185–192 (2005).
47. A. Schulz, J. Jankowski, W. Zidek, V. Jankowski, Absolute quantification of endogenous angiotensin II levels in human plasma using ESI-LC-MS/MS. *Clin. Proteomics* **11**, 37 (2014).
48. Y. Zou, H. Akazawa, Y. Qin, M. Sano, H. Takano, T. Minamino, N. Makita, K. Iwanaga, W. Zhu, S. Kudoh, H. Toko, K. Tamura, M. Kihara, T. Nagai, A. Fukamizu, S. Umemura, T. Iiri, T. Fujita, I. Komuro, Mechanical stress activates angiotensin II type 1 receptor without the involvement of angiotensin II. *Nat. Cell Biol.* **6**, 499–506 (2004).
49. H. Zheng, H. H. Loh, P.-Y. Law, β-Arrestin-dependent μ-opioid receptor-activated extracellular signal-regulated kinases (ERKs) translocate to nucleus in contrast to G protein-dependent ERK activation. *Mol. Pharmacol.* **73**, 178–190 (2008).

50. M. Aplin, G. L. Christensen, M. Schneider, A. Heydorn, S. Gammeltoft, A. L. Kjølbye, S. P. Sheikh, J. L. Hansen, Differential extracellular signal-regulated kinases 1 and 2 activation by the angiotensin type 1 receptor supports distinct phenotypes of cardiac myocytes. *Basic Clin. Pharmacol. Toxicol.* **100**, 296–301 (2007).
51. R. P. Vieira, T. Müller, M. Grimm, V. von Gernler, B. Vetter, T. Dürk, S. Cicko, C. K. Ayata, S. Sorichter, B. Robaye, R. Zeiser, D. Ferrari, A. Kirschbaum, G. Zissel, J. C. Virchow, J.-M. Boeynaems, M. Idzko, Purinergic receptor type 6 contributes to airway inflammation and remodeling in experimental allergic airway inflammation. *Am. J. Respir. Crit. Care Med.* **184**, 215–223 (2011).
52. A. Shotan, J. Widerhorn, A. Hurst, U. Elkayam, Risks of angiotensin-converting enzyme inhibition during pregnancy: Experimental and clinical evidence, potential mechanisms, and recommendations for use. *Am. J. Med.* **96**, 451–456 (1994).
53. O. Gribouval, M. Gonzales, T. Neuhaus, J. Aziza, E. Bieth, N. Laurent, J. M. Bouton, F. Feuillet, S. Makni, H. Ben Amar, G. Laube, A.-L. Delezoide, R. Bouvier, F. Dijoud, E. Ollagnon-Roman, J. Roume, M. Joubert, C. Antignac, M. C. Gubler, Mutations in genes in the renin-angiotensin system are associated with autosomal recessive renal tubular dysgenesis. *Nat. Genet.* **37**, 964–968 (2005).
54. C. R. Esther Jr., T. E. Howard, E. M. Marino, J. M. Goddard, M. R. Capecchi, K. E. Bernstein, Mice lacking angiotensin-converting enzyme have low blood pressure, renal pathology, and reduced male fertility. *Lab. Invest.* **74**, 953–965 (1996).
55. K. Nishioka, M. Nishida, M. Ariyoshi, Z. Jian, S. Saiki, M. Hirano, M. Nakaya, Y. Sato, S. Kita, T. Iwamoto, K. Hirano, R. Inoue, H. Kurose, Cilostazol suppresses angiotensin II–induced vasoconstriction via protein kinase A–mediated phosphorylation of the transient receptor potential canonical 6 channel. *Arterioscler. Thromb. Vasc. Biol.* **31**, 2278–2286 (2011).
56. S. Koizumi, Y. Shigemoto-Mogami, K. Nasu-Tada, Y. Shinozaki, K. Ohsawa, M. Tsuda, B. V. Joshi, K. A. Jacobson, S. Kohsaka, K. Inoue, UDP acting at $P2Y_6$ receptors is a mediator of microglial phagocytosis. *Nature* **446**, 1091–1095 (2007).
57. K. Arai, Y. Maruyama, M. Nishida, S. Tanabe, S. Takagahara, T. Kozasa, Y. Mori, T. Nagao, H. Kurose, Differential requirement of $G\alpha_{12}$, $G\alpha_{13}$, $G\alpha_q$, and $G\beta\gamma$ for endothelin-1-induced c-Jun NH_2-terminal kinase and extracellular signal-regulated kinase activation. *Mol. Pharmacol.* **63**, 478–488 (2003).

Acknowledgments: We thank N. A. Lambert (Georgia Regents University) for the gift of BRET plasmids (Venus-PM). We also thank T. Shigematsu for technical support. **Funding:** This work was supported by grants from the Japan Science and Technology Agency, the Precursory Research for Embryonic Science and Technology Program (to M.N.); Grants-in-Aid for Scientific Research (no. 25293018 to M.N.; no. 15K18883 to A.N.) and Platform for Drug Discovery, Informatics, and Structural Life Science (to K.I.) from the Ministry of Education, Culture, Sports, Science and Technology, Japan; Kimura Memorial Heart Foundation, Daiko Foundation, and Novartis Foundation (Japan) for the Promotion of Science (to M.N.). **Author contributions:** A.N., C.S., and M.N. designed the project; A.N., C.S., H.T.-S., T.S., and T.N.-T. performed experiments; K.H., T.I., M.T., H.K., K.I., J.-M.B., and B.R. contributed reagents/analytic tools; A.N. and M.N. wrote the manuscript. All authors discussed the results and commented on the manuscript. **Competing interests:** The authors declare that they have no competing interests. **Data and materials availability:** The *$P2Y_6R^{(-/-)}$* mice require a material transfer agreement from the Institute of Interdisciplinary Research, Belgium.

Submitted 29 June 2015
Accepted 29 December 2015
Final Publication 19 January 2016
10.1126/scisignal.aac9187
Citation: A. Nishimura, C. Sunggip, H. Tozaki-Saitoh, T. Shimauchi, T. Numaga-Tomita, K. Hirano, T. Ide, J.-M. Boeynaems, H. Kurose, M. Tsuda, B. Robaye, K. Inoue, M. Nishida, Purinergic $P2Y_6$ receptors heterodimerize with angiotensin AT1 receptors to promote angiotensin II–induced hypertension. *Sci. Signal.* **9**, ra7 (2016).

Science Signaling

Purinergic $P2Y_6$ receptors heterodimerize with angiotensin AT1 receptors to promote angiotensin II–induced hypertension

Akiyuki Nishimura, Caroline Sunggip, Hidetoshi Tozaki-Saitoh, Tsukasa Shimauchi, Takuro Numaga-Tomita, Katsuya Hirano, Tomomi Ide, Jean-Marie Boeynaems, Hitoshi Kurose, Makoto Tsuda, Bernard Robaye, Kazuhide Inoue and Motohiro Nishida

Sci. Signal. **9** (411), ra7.
DOI: 10.1126/scisignal.aac9187

Raising blood pressure with age

Activation of angiotensin AT1 receptors in vascular smooth muscle cells by angiotensin II can trigger either proliferation or hypertrophy (the latter of which increases blood pressure), depending on age. Nishimura *et al.* discovered that an age-related increase in the heterodimerization of AT1 receptors with purinergic $P2Y_6$ receptors explained the different responses to angiotensin II. Blood pressure increased to a lesser extent in response to angiotensin II in mice lacking $P2Y_6$ receptors. Vascular smooth muscle cells from young mice had less $P2Y_6$ receptor than those from older mice. Angiotensin II increased the proliferation of vascular smooth muscle cells from young mice but increased cell size in those from older mice by activating different signaling pathways. Thus, targeting the interaction between AT1 and P2Y6 receptors may decrease age-associated high blood pressure.

Science Signaling (ISSN 1937-9145) is published by the American Association for the Advancement of Science, 1200 New York Avenue NW, Washington, DC 20005. The title *Science Signaling* is a registered trademark of AAAS.